

# Medium Access Control Protocol Design for Sensors Powered by Wireless Energy Transfer

Prusayon Nintanavongsa, M. Yousof Naderi, and Kaushik R. Chowdhury

Dept. of Electrical and Computer Engineering,  
Northeastern University, Boston, Massachusetts 02115  
Email: {prusayon, naderi, krc}@ece.neu.edu

**Abstract**—Wireless transfer of energy will help realize perennially operating sensors, where dedicated transmitters replenish the residual node battery level through directed radio frequency (RF) waves. However, as this radiative transfer is in-band, it directly impacts data communication in the network, requiring a fresh perspective on medium access control (MAC) protocol design for appropriately sharing the channel for these two critical functions. Through an experimental study, we first demonstrate how the placement, the chosen frequency, and number of the RF energy transmitters affect the sensor charging time. These studies are then used to design a MAC protocol called RF-MAC that optimizes energy delivery to desirous sensor nodes on request. To the best of our knowledge, this is the first distributed MAC protocol for RF energy harvesting sensors, and through a combination of experimentation and simulation studies, we demonstrate 112% average network throughput improvement over the modified unslotted CSMA MAC protocol.

**Index Terms**—RF harvesting, Optimization, Medium Access Protocol, Sensor, Wireless power transfer, 915 MHz.

## I. INTRODUCTION

Wireless energy transfer will allow deployed sensors to recharge during network operation, thereby extending their lifetimes and minimizing application downtime. Our recent research on powering Mica2 sensor motes by harvesting the energy contained in radio frequency (RF) electromagnetic waves in [1] indicated the potential for large scale deployment of this technology. However, at the protocol level, this form of in-band energy replenishment is fraught with several challenges on (i) how and when should the energy transfer occur, (ii) its priority over, and the resulting impact on, the data communication, (iii) the challenges in aggregating the charging action of multiple transmitters, and (iv) impact of the choice of frequency. Thus, the act of energy transfer becomes a complex medium access problem, which must embrace a cross-disciplinary approach incorporating wave propagation effects and device characteristics, apart from the classical link layer problem of achieving fairness in accessing the channel. This paper is concerned with a design of a CSMA/CA based MAC protocol for such RF energy harvesting sensors, inspired by experimental evaluations on our testbed.

An example network architecture, with stationary, omnidirectional energy transmitters (ETs)  $x$ ,  $y$ , and  $z$ , is shown in Figure 1(a). The sensor  $S1$  can be charged either through a unilateral action of any of the ETs, or through a coordinated transmission of multiple ETs. Interestingly, the joint action can

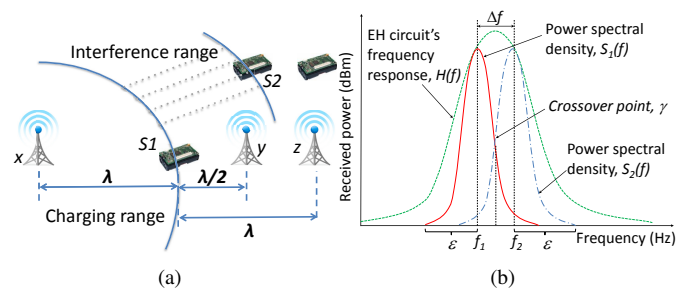


Fig. 1. Network architecture with energy transmitters ( $x, y, z$ ) and harvesting sensors ( $S1, S2$ ) (a) Two-tone wireless energy transfer (b)

only be beneficial if the arriving waves at sensor  $S1$  are aligned in phase. Hence, ETs  $x$  and  $z$  may together transmit, both being at a multiple of the signal wavelength  $\lambda$  away (which translates in a phase difference that results in ‘constructive’ interference). While the sensor can also be charged by ET  $y$ , combining the action of  $y$  with either of the others diminishes the performance (owing to  $y$  causing ‘destructive’ interference with respect to  $x$  and  $z$ ).

Our MAC protocol that works with RF energy harvesting, called as RF-MAC, ensures optimal energy delivery to the requesting node. In RF-MAC, a node broadcasts its request for energy (RFE) packet containing its ID, and then waits to hear for the ETs in the neighborhood. These responses from ETs are called cleared for energy (CFE) pulses, which are simple, time-separated energy beacons. These pulses may be transmitted by more than one ET concurrently, as overlapping CFEs need not be distinguished. Rather, the concurrent emission of the CFEs increases the received energy level at the sensor, and this indicates a higher number of potential transmitters from the energy requesting sensor. The responding ETs are then classified into two sets, based on rough estimates of their separation distance from the energy requesting node to minimize the impact of destructive interference as much as possible. Each set of ETs is assigned a slightly different peak transmission frequency (separated by only few KHz, hence still called in-band as the channel separation is typically 5 MHz for 802.11) so that each set contributes constructively to the level of RF energy received at the node. The core contributions of our work can be summarized as follows:

- We experimentally identify the operating constraints of the RF energy transferring MAC protocol using actual wireless energy harvesting circuits interfaced with Mica2 motes. We demonstrate how two slightly separated energy transfer frequencies can be assigned to ETs to improve the constructive interference of their collective action.
- We formulate the optimality conditions for the energy transfer, and create a strongly coupled protocol that operates on link layer metrics with the awareness of both the underlying hardware and fundamental limits of RF energy harvesting.

The rest of this paper is organized as follows: In Section II, we give the related work. Section III describes preliminary experiments used to motivate and design the RF-MAC protocol detailed in Section IV. The simulation results are presented in Section V. Finally, Section VI concludes our work.

## II. RELATED WORK

MAC protocols that aim for energy conservation have been extensively explored in the recent past, with a comprehensive classification and survey on this topic presented in [3]. Specific to the scenario of RF energy transfer, the protocol proposed in [4], and its subsequent analytical model in [5], adopts a duty-cycle based on the proportion of harvested energy. However, this protocol requires a strict centralized base station control and relies on out-of-band RF power transfer, which does not result in the added complexity we observe in our in-band case. In [6], the authors evaluate conventional MAC protocols, such as the classical TDMA and variants of ALOHA under a packet deliverability metric, assuming again out-of-band RF transfer. A CSMA-based MAC protocol with ARQ error control mechanism is modeled in [10] leveraging stochastic semi-markov models. In [7], the authors present multiple concepts for multi-hop wireless energy transfer (such as store and forward vs. directly single hop transfer) and derive the efficiency of each method using inductive coupling first demonstrated in [8]. However, this non-radiative transfer is shown to work up to 2 m and requires perfectly aligned coils of 25 cm radius among the source and receiver nodes, not feasible in a randomly deployed network. RFID technology comes closest to the energy transferring paradigm, where a tag operates using the incident RF power emitted by the transmitter [9]. However, there are limitations in directly porting these approaches to networking scenarios since RFID is unable to generate enough energy to run the local processing tasks on the node, such as powering the Atmel ATmega128L micro-controller on the Mica2 mote [11].

## III. PRELIMINARY EXPERIMENTS

In our experiments to characterize the constructive and destructive effect of the ETs, we placed two such 0 dBm continuous wave transmitters 2.5 m away from the receiver. Two Agilent N5181 MXG RF signal generators, each connected to a  $50\Omega$  omnidirectional antenna tuned to the 915 MHz ISM band, were used to generate the signal. We fixed the phase of one signal generator and varied the phase of another signal

generator, while keeping their locations fixed (note that keeping the transmission phase fixed and varying their distance as a function of the signal wavelength will have the same effect on the received signal phase). The fall in the signal strength was dramatic when the ETs operated in phase opposition ( $-54$  dBm) compared to in-phase operation ( $-36$  dBm).

The bandwidth of the RF energy harvesting circuit connected to the sensor determines the maximum frequency separation of the continuous wave ETs, refer to Figure 1(b). If the bandwidth of this circuit is narrow, or the spread of the transmitted spectrum too large, there may not be enough room to completely separate the spectrum of the two transmitters by assigning them slightly varying center-frequencies. Hence, there may be an overlap in the two out-of-phase energy transmitters with a resulting destructive combination. Moreover, the bandwidth of the energy transmitter also has an effect on maximum energy transfer. It is preferable to have signal power contained in a narrow bandwidth, say within 99% of the occupied bandwidth. This relaxes the constraint of having a complete separation of out-of-phase signal bandwidth for different ETs.

Having established the need for separating out-of-phase ETs, we next direct our attention on how much of the phase mismatch is actually harmful. If the ETs are not completely  $\pi$  radians separated in phase, then some of them may even be allowed to transmit together. The resultant increase in the raw emitted power in these cases compensates for the loss owing to the slight mismatch. The phase difference  $\Delta\phi$  between two energy transmitters is varied from  $[0, \pi]$  radians in order to study its effect on the received signal power at 915 MHz. A phase difference of 0 or  $2\pi$  for the received signal (the emitted signals being in-phase) corresponds to a linear distance of one wavelength between the two transmitters. Thus, depending upon the actual distance  $L$  between the ET  $x$  and receiver node, we represent  $\phi_x = \frac{L}{\lambda} \cdot 2\pi$ . Here,  $\lambda$  is the wavelength of the transmitted radiation. We observe that for small phase difference, i.e., for  $\Delta\phi \leq \frac{\pi}{2}$ , the resultant signal strength is not significantly lowered (i.e., the fall is only about  $1 - 2$  dBm). Hence, we group together all those ETs that are separated by  $\Delta\phi \leq \frac{\pi}{2}$  under one category (and center its transmissions at frequency  $f_1$ , say). Similarly, ETs that are separated by  $\frac{\pi}{2} \leq \Delta\phi \leq \pi$  fall in the second category (and use frequency  $f_2$  as the center transmission). We call this method as the *two-tone* energy transfer.

In Figure 1(b), using the discussion above on the relationship between the phase and distance, all ETs separated by a multiple of the wavelength from each other, i.e.,  $L = m\lambda$ ,  $m = 1, 2, \dots$  transmit on  $f_1$ , while the others separated by  $L = (m + 1/2)\lambda$  transmit on frequency  $f_2$ . As there are two active transmission tones present concurrently during transmission, each of these are separated in the frequency domain, one on each side of the center response point of the harvesting circuit. Both these tones must be completely encompassed by the response of the harvesting circuit at the receiver side. Clearly, the EH circuit with a wide and flat frequency response accommodates better separation of

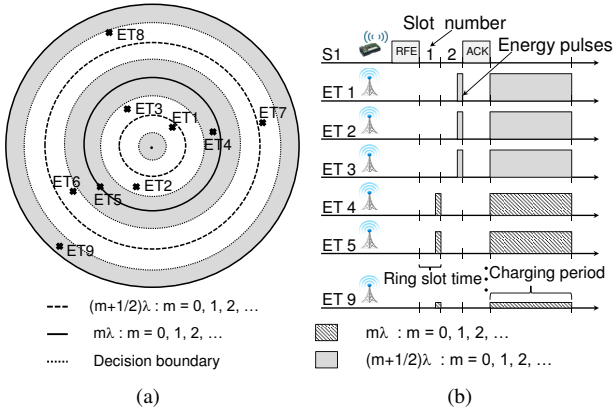


Fig. 2. Energy transmitter selection (a) Timing diagram for RF-MAC (b)

transmitting frequencies. Our detailed investigations on the design of such a RF energy harvesting circuit are described in [1], where we design the circuit to deliver the highest power at the tuned frequency of 900 MHz. However, the output power begins to drop if there is any deviation from the tuned frequency, depending upon component selection and normal wear and tear of continuous operation. We measured the reduction in circuit efficiency within a frequency span of 10 MHz on either side of 900 MHz and observed that the reduction is approximately 0.38%. As opposed to this, the 99% occupied bandwidth of the Powercaster transmitter is relatively small, approximately 63 kHz, thereby allowing us to accommodate the entire transmission spectrum of the ET within the frequency response curve of the EH circuit.

#### IV. RF-MAC PROTOCOL DESCRIPTION

Recall that energy contained within a capacitor of value  $C$  and the voltage across its terminals are related as  $E_{res} = \frac{1}{2}CV^2$ . When the voltage falls below a pre-set threshold ( $\sim 2.3v$ , as minimum operating voltage of the Mica2 is 1.8v), the node sends out the RFE packet, requesting for energy. The RFE contains only the requesting sensor node's ID, transmitted at a constant signal strength. This RFE can only be sent when the channel is free, i.e., when there is no ongoing data transfer or energy charging operation and the channel lies idle for the DIFS duration. The ETs that receive this packet estimate roughly their distances from the node, based upon the received signal strength (RSS). Recall from Section III, the distance between the ET and the sensor node directly results in a phase difference for the incoming wireless signals at the node. The ETs that identify themselves to lie in the band  $[m\lambda - \frac{\lambda}{4}, m\lambda + \frac{\lambda}{4}]$ , are grouped together, where  $m = \{1, 2, \dots\}$ . We call this as Group I. Similarly, the other ETs in the range  $[(m+1/2)\lambda - \frac{\lambda}{4}, (m+1/2)\lambda + \frac{\lambda}{4}]$  fall in the second group, called Group II. Thus, on receiving the RFE, each ET knows which concentric band it lies in centered around the requesting node, and the group in which it belongs. Figure 2(a) shows a sample scenario. The shaded region depicts the ETs 4 and 5 that lie in the band of  $\lambda$ , i.e., in Group I. This region extends up to  $\frac{\lambda}{4}$  on either side of the central bold line

that lies at an exact distance of  $\lambda$  with the requesting node placed at the center. Since we do not precisely require the ET to calculate the distance from the requesting node, but only need to determine if it lies within a concentric band-region, our approach is more robust to RSS fluctuations. Of course, using a dedicated localization scheme or GPS hardware considerably eases this constraint, though adding to the implementation cost and power requirement.

1) *Grouping of the responding ETs:* The ETs that hear the RFE reply back with a single, constant energy pulse. Each concentric band has the choice of one of two time slots in which this pulse may be emitted, beginning from the instant of completion of the RFE, as shown in Figure 2(b). Referring again to the band structure in Figure 2(a), the first slot is allocated for CFE pulses sent by energy transmitter of Group I (note: all Group I bands are shown shaded). Similarly, CFE pulses from energy transmitters of Group II are sent during the second slot, i.e. ETs 1, 2 and 3 collectively lie in the second concentric (Group II) band and simultaneously transmit their pulses in the second slot. The node that sent the initial RFE estimates the total energy that it will receive based on the signal strength of the CFE pulses in the slot number in which they were received. This arrangement of using the pulses allows the ETs to be simple in design, and removes the concern of collisions in the reply packet. Unlike classical data communication, it is not important for the node to know *which* ET will transmit energy. Rather, its energy calculations are based on *how much* energy is contributed by the two groups of ETs separately. We define this cumulative energy as  $E_{RX}^{Group I}$  and  $E_{RX}^{Group II}$ , respectively, which are calculated by the RFE issuing node from the received pulses. Each slot time is  $10 \mu s$  in our work, allowing a very fast response time.

The purpose of differentiating the energy contribution from the two groups is useful in the next stage, where an optimization function returns the center frequencies of the ETs. Let Group I ETs be centered at frequency  $f_1$ , and Group II ETs be centered at frequency  $f_2$  so that they can concurrently transfer energy without destructively affecting each other. Also, a desirable goal is to have minimum separation  $f_2 - f_1$ , as the spectrum is most efficiently utilized. This also leaves open the possibility of future advancements using more than two concurrent frequencies. How to select these frequencies  $f_1$  and  $f_2$  is explained next, which takes into account two important physical layer characteristics of the energy transfer. The first is the spectrum response of the energy harvesting circuit that is connected to the sensor nodes, shown by the envelope  $H(f)$  in the frequency domain in Figure 1(b). The power spectral density (PSD) of the two groups of ETs is the other concern, represented by  $S_1(f)$  and  $S_2(f)$ , respectively, for Group I and Group II. These shapes are observed by the sensor node from the incoming pulses from the ETs. Thus, the bandwidth  $2\epsilon$  of the transmission spectrum (centered at  $f_1$  and  $f_2$ ) must be selected in such a way their is minimum overlap between their individual spectra, and yet contained within the envelope of  $H(f)$  to affect the maximum level of power transfer. We use the following optimization assuming

the transmission spectrum of the ETs occupies a bandwidth of  $2\epsilon$ .

2) *Optimization function for frequency assignment*: The aim of the optimization formulation is to maximize the energy transfer  $E_{RX}^{Max} = E_{RX}^{Group I} + E_{RX}^{Group II}$  to the requesting sensor node. The energy transferred by the RF signal at a given frequency point is the product of the power spectral density and the circuit frequency response, i.e.,  $S_{1/2}(f)H(f)$ . Thus, the useful components that need to be maximized are the first two terms of (2), which give the constructive energy contribution of the ETs of the two groups.

Given :  $S_1(f)$ ,  $S_2(f)$ , and  $H(f)$

To find :  $f_1, f_2$  (1)

To Maximize :

$$E_{RX}^{Max} = \int_{f_1-\epsilon}^{f_1+\epsilon} S_1(f)H(f)df + \int_{f_2-\epsilon}^{f_2+\epsilon} S_2(f)H(f)df - \underbrace{\left( \int_{f_2-\epsilon}^{\gamma} S_2(f)H(f)df + \int_{\gamma}^{f_1+\epsilon} S_1(f)H(f)df \right)}_{\text{destructive interference}} \quad (2)$$

Subject to :

$$\left. \frac{d(S_1(f)H(f))}{df} \right|_{f=\gamma} < 0 \quad (3)$$

$$\left. \frac{d(S_2(f)H(f))}{df} \right|_{f=\gamma} > 0 \quad (4)$$

The two constraints of the above optimization ensure that the spectrum shapes of the Group I and Group II ETs does not overlap completely. We assign  $f_1$  to the left of  $f_2$  on the frequency scale (see Figure 1(b)). At the point of the intersection of the PSD curves  $S_1(f)$  and  $S_2(f)$ , which we call the *cross-over* point  $\gamma$ , the slope of the curves must be positive and negative, respectively. This is calculated by differentiating the respective PSD plots at  $\gamma$ , to ensure that one of them increases (positive slope) while the other falls (negative slope).

A problem is said to have an optimal substructure if an optimal solution can be constructed efficiently from optimal solutions to its sub-problems. We claim that our proposed optimization also exhibits the optimal substructure property.

With the resulting dual-frequency wireless energy transfer, both groups of ETs can be simultaneously active. The final part of this stage involves letting the ETs know that they are cleared for energy transmission through an Acknowledgement (ACK) packet. This packet provides the ETs the center point for the frequencies  $f_1$  and  $f_2$ , according to the optimization results. The ETs know which group they belong to internally, based on the RSS-based band structure shown in Figure 2(a). After a short SIFS wait period following the ACK, the ETs begin their transmission. In case of loss of the RFE due to packet collision or bad channel conditions, the contention windows are reset to the minimum width, thereby initiating an immediate subsequent retry.

## V. SIMULATION RESULTS

In this section, we thoroughly evaluate our proposed MAC protocol using the ns-2 simulator. We observe the behavior

of RF-MAC protocol with respect to the number of energy transmitters and the numbers of nodes. The simulation parameters are set as follows: The EH circuit parameters are from [1]. We model the ETs on the Powercaster transmitter [2], which radiates continuous waves at 3 W. The operational characteristics of the sensor, such as energy spent in transmission, reception, idle listening, channel bandwidth, etc. are from MICA2 specifications [11]. Additional parameters used in the simulation are present in Table I. Unless specifically stated, 250 sensor nodes and 100 ETs are deployed uniformly at random in  $50 \times 50 m^2$  grid. The default packet size is 50 Bytes and the sender/receiver pairs are chosen randomly from the set based on the random number generator in ns-2.

We compare the proposed RF-MAC with the modified unslotted CSMA. RF-MAC has the frequency optimization and ET selection features by assigning different frequencies to the two groups of ETs. The unslotted CSMA modified from the description in [3] provides the base case and reference protocol for comparison. Here, each sensor node may issue the RFEs and receive the CFEs. However, there is no attempt to assign optimal frequency to the ETs.

### A. Impact of the number of ETs

In this sub-section, we investigate the effect of the number of ETs on the average harvested energy and average network throughput for different MAC protocols. Figure 3 shows the effect of the ET density on the average harvested energy of RF-MAC. The ET density, defined as the average number of ETs located within node's radio range, is varied from 1 to 12. It is clear that RF-MAC delivers monotonically increasing average harvested energy with increasing the number of ET density. The benefit of the frequency optimization greatly improves the performance as it maximizes the energy transfer by separating the two transmission spectrum and ensuring the highest level of energy delivery. Without this optimization, ETs enter the charging process and do not take into account the possibility of destructive interference, resulting in sub-optimal energy transfer.

The average network throughput is shown in Figure 4 and the pattern resembles to that of the average harvested energy plot. RF-MAC yield higher average network throughput as ET density increases. Both the average harvested energy and average network throughput of unslotted CSMA are lower. This is because the unslotted CSMA does not have the frequency optimization feature offered by the RF-MAC protocol. In this case, RF-MAC yields over 89% and 112% more than the unslotted CSMA in terms of the average harvested energy and average network throughput, respectively.

### B. Impact of the number of sensor nodes

We investigate how RF-MAC protocol behaves when the number of sensor nodes in the topology changes. We randomly deploy various numbers of sensor nodes in the topology, ranging from 60 to 240. The average harvested energy is shown in Figure 5, wherein the performance of RF-MAC smoothly tends to stabilize and unslotted CSMA has a rather

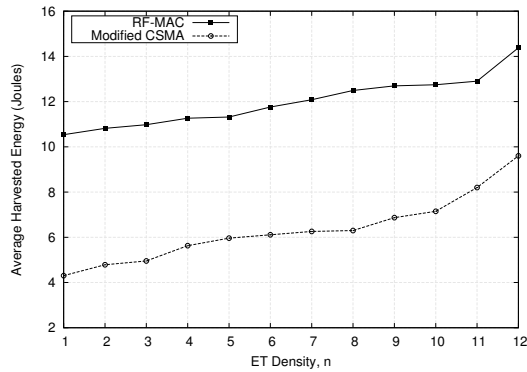


Fig. 3. Effect of the number of ETs on average harvested energy

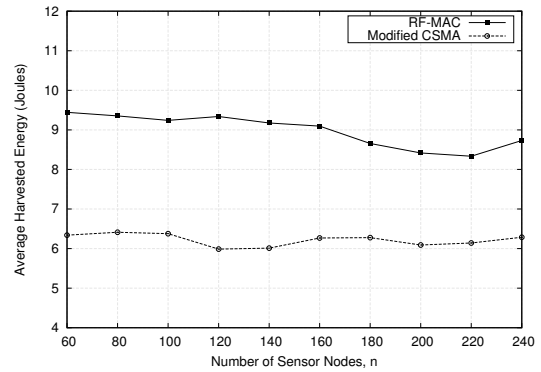


Fig. 5. Effect of the number of nodes on average harvested energy

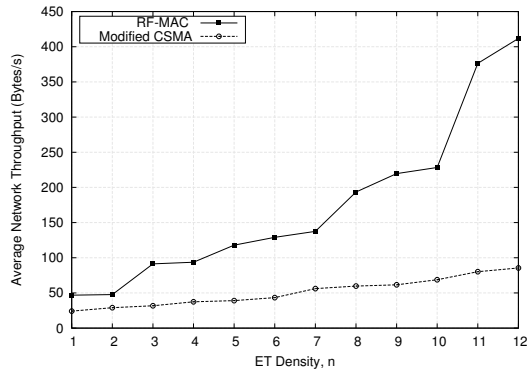


Fig. 4. Effect of the number of ETs on average network throughput

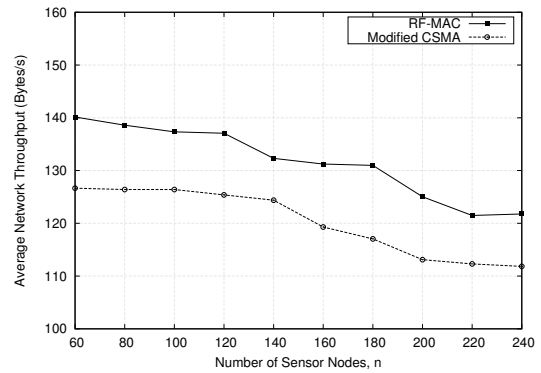


Fig. 6. Effect of the number of nodes on average network throughput

constant average harvested energy with fluctuation around the mean trend. Again, RF-MAC offers higher average harvested energy when compared to modified CSMA scheme. Figure 6 depicts the average network throughput of RF-MAC with different numbers of sensor nodes. Similar to the earlier case, the unslotted CSMA performs lower than RF-MAC in terms of average network throughput.

## VI. CONCLUSIONS

The RF-MAC protocol defines new metrics and methods for selection of RF energy transmitters or ETs, that ensures high lifetime of the sensor nodes. The grouping of the ETs into two sets with varying transmission frequencies, and the minimal control overhead are both geared to keep the hardware requirements simple, and the protocol easy to implement. Simulation results reveal that RF-MAC largely outperforms the unslotted CSMA in both average harvested energy and average network throughput. The features incorporated in RF-MAC efficiently optimize the energy delivery.

## ACKNOWLEDGMENT

This material is based upon work supported by the US National Science Foundation under Grant No. CNS-1143681.

## REFERENCES

- [1] P. Nintanavongsa, U. Muncuk, D. R. Lewis, and K. R. Chowdhury, Design Optimization and Implementation for RF Energy Harvesting Circuits. *IEEE Journal on Emerging and Selected Topics in Circuits and Systems*, vol. 2, no. 1, pp. 24–33, Mar. 2012.
- [2] Powercast Corporation, Lifetime Power Evaluation and Development Kit. [Online] <http://www.powercastco.com/products/development-kits/>
- [3] Z. A. Eu, H.P. Tan, and W. K. G. Seah, Design and performance analysis of MAC Schemes for Wireless Sensor Networks Powered by Ambient Energy Harvesting. *Ad Hoc Networks*, vol. 9, no. 3, pp. 300–323, 2011.
- [4] J. Kim and J. W. Lee, Energy Adaptive MAC Protocol for Wireless Sensor Networks with RF Energy Transfer. *Proc. of IEEE Intl. Conference on Ubiquitous and Future Networks (ICUFN)*, pp. 89–94, 2011.
- [5] J. Kim and J. W. Lee, Performance Analysis of the Energy Adaptive MAC Protocol for Wireless Sensor Networks with RF Energy Transfer. *Proc. of IEEE Intl. Coverage and Transmission Conference (ICTC)*, pp. 14–19, 2011.
- [6] F. Iannello, O. Simeone, and U. Spagnolini, Medium Access Control Protocols for Wireless Sensor Networks with Energy Harvesting. *IEEE Transactions on Communications*, vol. 60, no.5, pp. 1381–1389, May. 2012.
- [7] M.K. Watfa, H. Al-Hassanieh, S. Selman, Multi-hop wireless energy transfer in WSNs. *IEEE Communication Letter*, vol. 15, no. 12, pp. 1255–1277, Oct. 2011.
- [8] A. Karalis, J. D. Joannopoulos, and M. Soljacic, Efficient wireless nonradiative mid-range energy transfer. *Annals of Physics*, vol. 323, no. 1, pp. 34–48, Jan. 2008.
- [9] J. Curty, M. Declercq, C. Dehollain, N. Joehl, Design and Optimization of Passive UHF RFID Systems, Springer, 2007.
- [10] M.Y. Naderi, S. Basagni, and K.R. Chowdhury, Modeling the Residual Energy and Lifetime of Energy Harvesting Sensor Nodes. *Proc. of IEEE Global Telecommunications Conference (GLOBECOM)*, pp. 3394–3400, Dec. 2012.
- [11] Crossbow Technology, Inc. [Online] <http://www.xbow.com/>